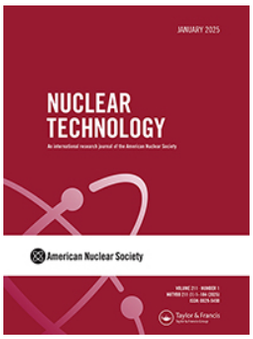

Nuclear Technology

ISSN: (Print) (Online) Journal homepage: www.tandfonline.com/journals/unct20

Evaluation of Fukushima Daiichi Unit 1 Ex-Vessel Phenomenon Leveraging on Primary Containment Vessel Robotic Inspections

Michal Cibula, Marco Pellegrini, Masato Mizokami & Shinya Mizokami

To cite this article: Michal Cibula, Marco Pellegrini, Masato Mizokami & Shinya Mizokami (07 Jun 2024): Evaluation of Fukushima Daiichi Unit 1 Ex-Vessel Phenomenon Leveraging on Primary Containment Vessel Robotic Inspections, Nuclear Technology, DOI: 10.1080/00295450.2024.2339578

To link to this article: https://doi.org/10.1080/00295450.2024.2339578

Published online: 07 Jun 2024.

NUCLEAR TECHNOLOGY

DOI: https://doi.org/10.1080/00295450.2024.2339578

Evaluation of Fukushima Daiichi Unit 1 Ex-Vessel Phenomenon Leveraging on Primary Containment Vessel Robotic Inspections

Michal Cibula,[a] Marco Pellegrini,[b] Masato Mizokami,[a] and Shinya Mizokami[a]*

[a]*Tokyo Electric Power Company Holdings, Inc., Tokyo, Japan*
[b]*The University of Tokyo, Tokyo, Japan*

Received February 15, 2024
Accepted for Publication March 31, 2024

Abstract — *The Great East Japan Earthquake and subsequent tsunami that struck the Fukushima Daiichi Nuclear Power Station gave ground to a set of events that resulted in an unprecedented severe accident occurring simultaneously in multiple reactors of one nuclear power station and significant release of radioactive materials into the environment. Following these events, Tokyo Electric Power Company in cooperation with domestic and international partners has made continuous efforts to clarify in detail the progression of the accident utilizing both analytical tools and robotic inspections of the damaged units. Recently, multiple inspections utilizing submersible remotely operated vehicles were conducted between December 2022 and March 2023, including the first entry into the pedestal area below the damaged reactor pressure vessel of Unit 1. This paper discusses the findings of these inspections in light of the evolving understanding of the accident scenario, leveraging insights gained through experimental and analytical studies on ex-vessel severe accident phenomena. The outcomes of these investigations have yielded new knowledge and highlighted existing gaps in our understanding. The identified knowledge gaps provide direction for future studies, ultimately advancing the level of nuclear safety.*

Keywords — *Fukushima Daiichi accident, unsolved issues, severe accident, molten core–concrete interaction, ex-vessel phenomena.*

Note — *Some figures may be in color only in the electronic version.*

I. INTRODUCTION

The Great East Japan Earthquake and subsequent tsunami that struck the Fukushima Daiichi Nuclear Power Station gave ground to a set of events that resulted in an unprecedented severe accident occurring simultaneously in multiple reactors of one nuclear power station and significant release of radioactive materials into the environment. Ever since then, Tokyo Electric Power Company (TEPCO), in cooperation with domestic and international partners, has been conducting numerous site investigations, as well as analyses, with the purpose of clarifying the current state inside the primary containment vessels (PCVs) and reactor pressure vessels (RPVs) of the damaged Units 1, 2, and 3.[1–3] Information obtained through these activities is essential for developing plans to achieve safe and successful progress of the decommissioning work. At the same time, the detailed clarification of accident progressions of the three units can bring more light to severe accident phenomena, resulting in improvement of nuclear safety for both operating and newly developed designs.[4]

Of the three units with damaged cores, Unit 1 experienced the earliest onset of severe accident, after losing all cooling functions practically immediately after the

*E-mail: mizokami.shinya@tepco.co.jp

tsunami arrival at the site and remained in the state without any effective cooling water injection for the longest period. This resulted in core damage and relocation of molten materials into the PCV. Investigation utilizing cosmic muon tomography indicated that there are no high-density substances (fuel) in the original position of the reactor core.[5] Because the operators did not have any practical means of intervention, it is considered that the drywell (D/W) at the time of the transition from the in-vessel phase to the ex-vessel phase did not hold any significant water inventory, except for small amounts of condensed water previously leaked from the RPV, which could accumulate in the sumps within the pedestal area and on the D/W floor to the level of about 20 cm at maximum.[6]

The above-mentioned events would give place to spreading of relocated materials and long-term unmitigated molten core–concrete interaction (MCCI) in a dry state, a phenomenon that has been extensively studied both experimentally and analytically. Because of the inherent limitations of experimental means and the complex nature of MCCI, it is generally agreed that there is room for improvement in understanding the relevant phenomena and the accuracy of currently available simulation codes.[7,8]

Benchmark studies focusing on both in-vessel and ex-vessel accident development have been successfully conducted within multiple Organisation for Economic Co-operation and Development/Nuclear Energy Agency (OECD/NEA) joint projects, pointing out some large discrepancies between the results of the analyses and the observed plant status. Some of the main identified uncertainties include the time and magnitude of events, such as corium relocation in the RPV and onto the cavity floor, and large and continuous progression of MCCI, among others.[9–11]

Figure 1 depicts the estimated state and fuel debris distribution within the PCV of Unit 1 based on the information acquired before 2022 (Ref. 6). With the purpose of collecting crucial information to grasp the state in the containment to efficiently proceed with the decommissioning work, as well as to further decrease the uncertainties related to the accident progression and severe accident phenomena understanding, a wide range of investigations inside the PCV utilizing submersible remotely operated vehicles (ROVs) was conducted between December 2022 and March 2023.

As a result, an extensive number of videos (exceeding 180 h) have been recorded, with short excerpts being available online[12–16] and the data in its entirety being available upon request at TEPCO's nuclear information

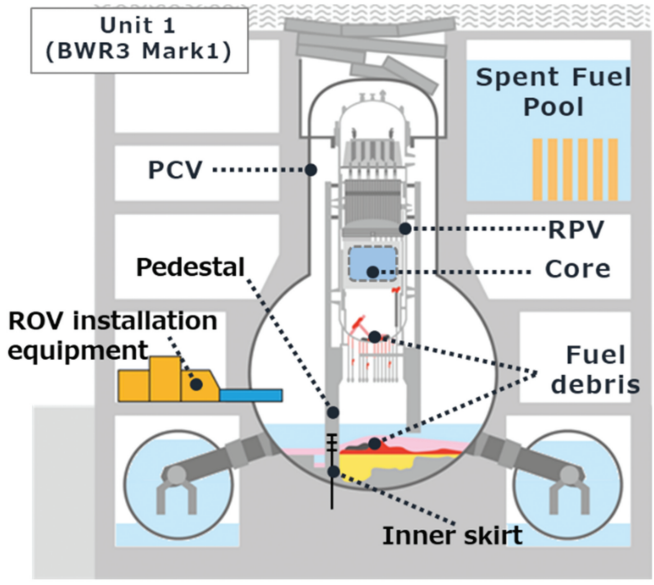

Fig. 1. Estimation of status inside RPV and PCV (as of 2022).

corner. The implications arising from these videos might be hard to grasp even for experts in the field, as these necessitate knowledge of the plant in order to correctly understand the position of the ROV throughout its investigation course, locations that are being captured, and in ideal cases their state prior to the accident in 2011. Hence, with this paper we aim to highlight the fundamental findings as the result of the inspection of Unit 1 and to point out added pieces of knowledge or, most of the time, inconsistencies with what has been believed by the severe accident research community. These inconsistencies represent a starting point for future directions in severe accident ex-vessel phenomena.

II. DRYWELL INVESTIGATION

The relatively high level of water accumulation in the D/W allowed use of submersible ROVs for the PCV internal investigation, with the purpose of information acquisition in the wide area of the D/W annulus and pedestal area. The ROV was inserted into the D/W from the west side of the ground floor (Fig. 2) and was subsequently lowered to the water surface reaching about 2 m high from the D/W floor. The investigation was conducted between January 2022 and March 2023 with focus on the state of equipment outside and inside of the pedestal area; distribution of deposits; fuel debris; and state of the pedestal wall, which supports the weight of the RPV and related structures. Information was collected outside of the pedestal approximately in the range

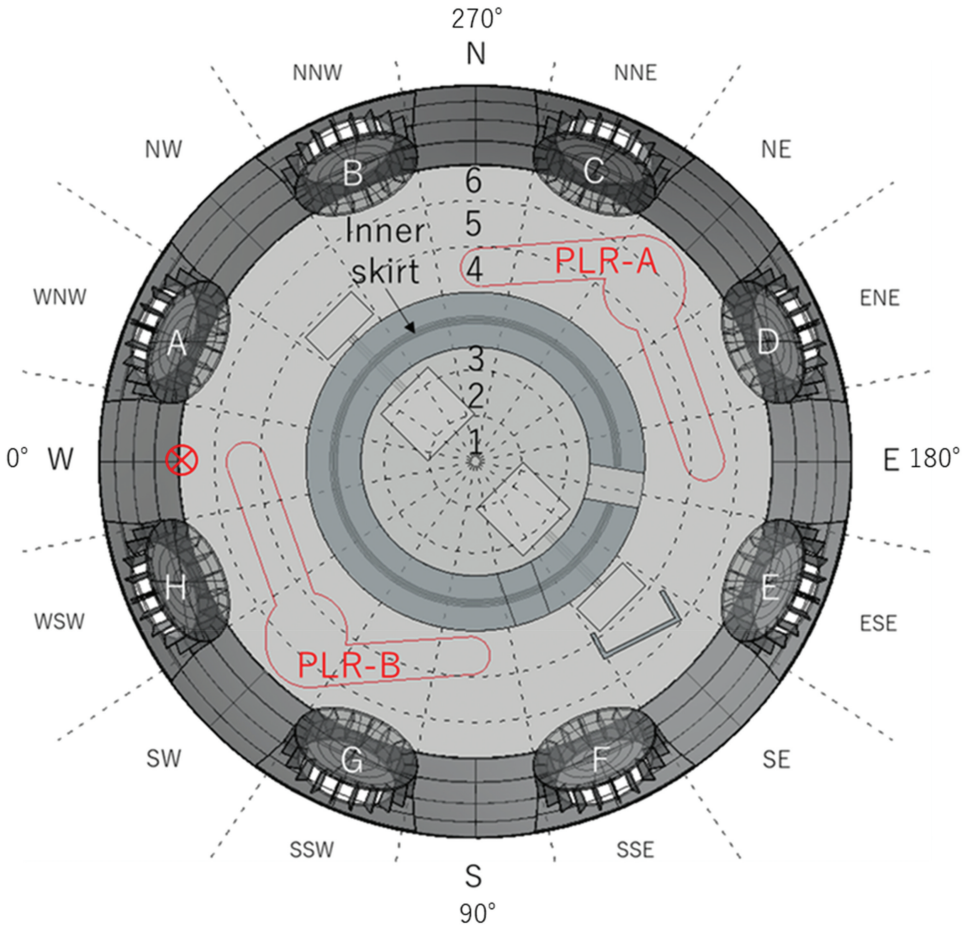

Fig. 2. Plane view of the D/W floor; cardinal directions and radial sections 1 through 6 used to indicate areas captured in the following figures; pedestal wall between sections 3 and 4; D/W floor pedestal opening in E-ESE direction; upper floor CRD exchange opening in SSE section. Red-colored lines denote outline of the PLR piping; rectangles in and outside of the pedestal area denote sump pits; white letters A through H denote jet deflectors; gray structure at SE-5 indicates shielding block; red circled X mark denotes ROV insertion point.

of W to NE) (0 to 215 deg) in the counterclockwise direction and inside the entire pedestal area with various degrees of detail depending on the accessibility by ROV. The obtained visual information from both under and above the water level is discussed considering the current knowledge of the ex-vessel severe accident phenomena with an attempt to identify knowledge gaps.

II.A. Observations in the Upper Pedestal Area

Practically no parts of the control rod drive (CRD) exchange equipment could be found, in contrast with Unit 2, where this equipment was found in its original position and only with minor damage (missing parts of the platform grating), and Unit 3, where although the CRD equipment itself was displaced from its original position, the rails, platform, and other parts could be identified. Perturbations on the water surface caused by dripping of the cooling water from the damaged lower head (LH) of the RPV were observed both in the central area and in the peripheral areas of the pedestal. Multiple cylindrically shaped objects were found leaning on the wall, particularly the N-3 and W-3 sections, which were identified as CRD and in-core monitor (ICM) housings detached from the RPV LH (Figs. 3, 4, and 5). In some cases, the flanges were in the upper position, meaning they turned upside down during their relocation (Fig. 6). Although the CRD housing support bars and hanger rods are displaced and/or deformed to a big extent, some of the displaced housings remain supported by them in a suspended position above the water level (or partially above the water level). The total number of confirmed relocated housings, including those suspended above water level, was more than 10. The schematic diagram of the CRD housings, their support structures, and pedestal wall can be seen in Fig. 7.

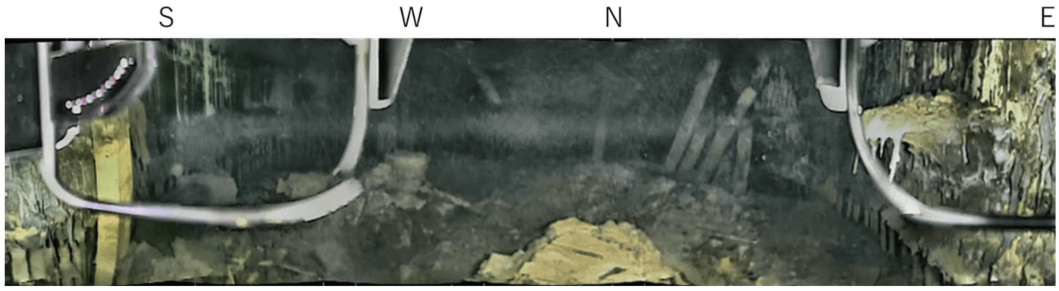

Fig. 3. Panoramic view of the pedestal area (taken from the pedestal opening).

Fig. 4. Fallen CRD housings leaning on the pedestal wall, severed on top and partially buried in deposits below (N-3).

Fig. 6. Fallen CRD housing leaning on the pedestal wall with flange in the upper position above the water level (NW-3).

Fig. 5. Detached ICM housing suspended above the water level (SE-3) near the pedestal wall.

In some instances, the severed sections of the CRD housings could be observed. CRDs consisting of several hollow cylinders inside the housings appear to have the gaps between each cylinder clogged by solidified materials (Fig. 8). Those completely separated from all the upper support structures have been found partially buried in the deposits, with some deformations and "gouging" on their surfaces, adherence of dark-colored material, and seemingly interfering with the protruding deposits attached to the pedestal wall (referred to as shelves) in the process of relocation, resulting in fracturing of the shelf in some instances.

High above the water level, numerous flanges of the CRD and ICM housings considered to be remaining in or near their original height could be observed. While their vertical position does not appear to be significantly changed, their positional relationship in the horizontal plane shows deviation from the original square grid (Fig. 9). A bundle of CRD and ICM housings was confirmed remaining in a slanted position with bulky deposits adhering to their surfaces. At least one of these housings is sticking out of this bundle farther downward and appears to be in contact with the end of the CRD exchange rail inside the opening in the higher part of the pedestal wall near 90 deg (Fig. 10).

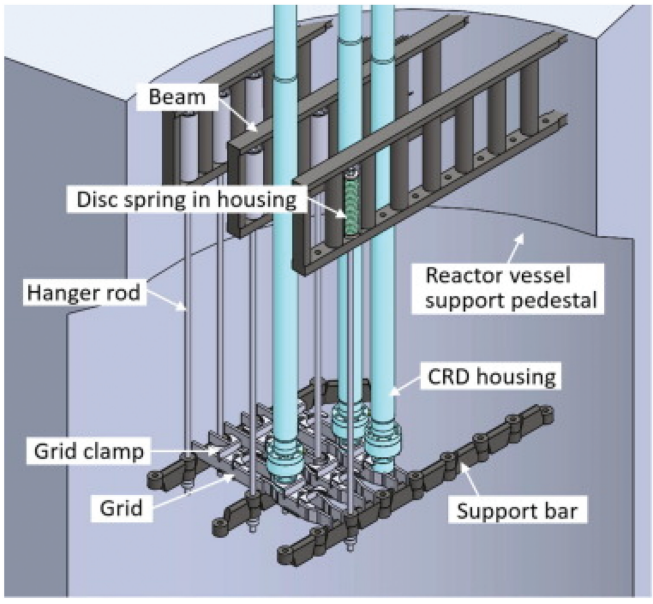

Fig. 7. Schematic diagram of CRD housings, support structures, pedestal wall, etc.[21]

II.B. Observations in the Lower Pedestal Area

Figure 3 shows the panoramic view of the pedestal area taken from the pedestal worker access opening (herein referred to as pedestal opening). Erosion of concrete along the entire inner circumference of the pedestal wall was confirmed up to the height of approximately 1 m. This left the vertical reinforcing steel rebars exposed, but surprisingly, no significant damage to the rebar itself was confirmed. In multiple locations where the extent of the concrete erosion and state of the rebars could be investigated in detail, the inner skirt could be observed as well. The inner skirt is a cylindrical reinforcing structure in the center of the pedestal wall reaching from the basemat up to the height of 1 m from the D/W floor (Figs. 1 and 2). No significant deformation of the inner skirt was confirmed either, and the concrete erosion is assumed to be reaching the center of the wall around the entire circumference of the pedestal inner wall.

Dark discoloration of the wall was observed above the areas with missing concrete up to the height of about 150 cm. At this height, protruding deposited materials of unknown nature (referred to as shelves), or discoloration suggesting their previous existence, were found in multiple areas. No significant abnormalities of the wall concrete were observed above this level, except for dark-colored materials adhering to some parts of the wall and accumulating on top of some shelves. The average height of the materials deposited on the pedestal area floor is assumed to be about 60 cm from the original floor level, with local maximum (in front of the pedestal opening) reaching to about 1.0 m. Figure 11 shows the simplified distribution of states of the pedestal

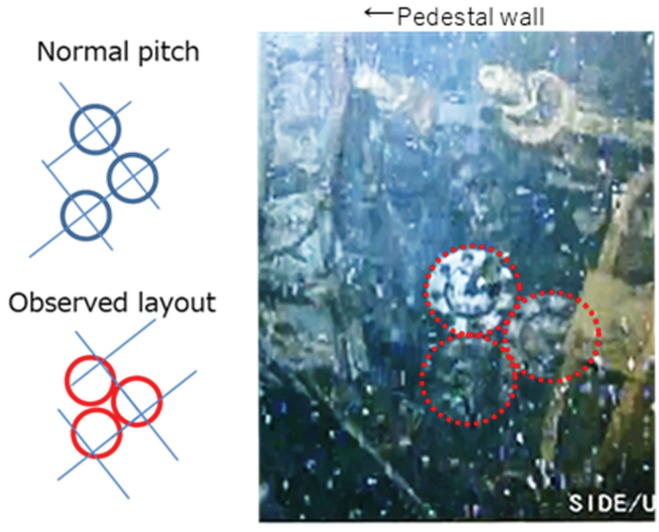

Fig. 9. Deviations of CRD housings from their normal pitch (ESE-3).

Fig. 8. Clogging of severed CRD housing (central section of the pedestal area) observed from below the severed section of the suspended CRD housing (right picture).

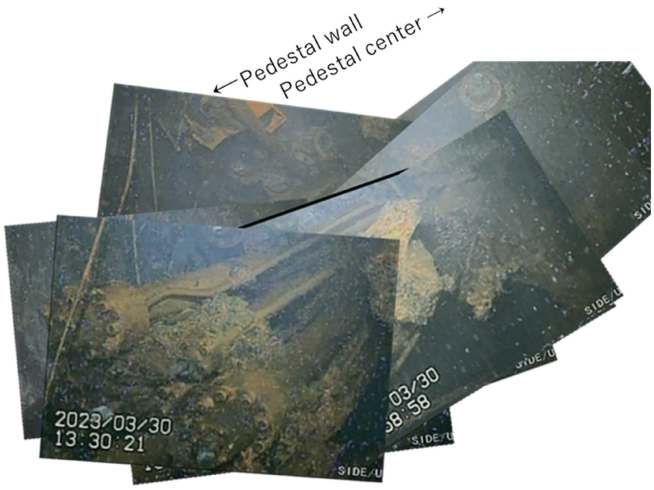

Fig. 10. Bulky deposits attached to the relocated CRD housings suspended above the water level (SSE-2 to SSE-3).

walls. No reactor internal structures (CRD housings considered to be ex-vessel structures) were identified in the pedestal area, unlike in the case of the other units,[17,18] where the upper tie plate of the fuel assembly (Unit 2), control rod guide tubes (Unit 3), and others could be found.

II.C. Observations in the Pedestal Opening

The damage to the pedestal wall concrete could be observed in the closest detail inside the pedestal opening (Fig. 12). The concrete of the pedestal wall was confirmed to be missing from both side walls of the opening, up to the height slightly exceeding the height of the inner skirt at maximum. No clear deformation of the inner skirt itself could be confirmed; however, the L-shaped rebars that are horizontally welded to the inner skirt to reinforce the corners of the opening were found bent on both inner and outer sides of the wall on both left and right sides of the opening. A slanted shelf is attached to the right side of the wall at the height of ~1.5 m on the pedestal inner corner and ~1.3 m on the outer corner. No shelf is currently attached to the left side of the wall; however, the discoloration and deterioration scale of the wall suggests the possibility of the previous existence of a slanted shelf similar to the one on the right side wall. In general, the distribution of the states along the walls of the pedestal opening is the same as inside the pedestal area, including the presence of dark-colored materials on top of and above the shelf. In addition, the piping of the reactor building closed cooling water system (RCW) serving to cool the equipment drain sump in the pedestal area could not be found in its original position along the left wall.

II.D. Observations Outside the Pedestal

On the outer wall of the pedestal, similarly as inside the pedestal area, missing concrete of the pedestal wall and exposed intact rebar have been confirmed. Because of the presence of the deposits and preexisting structures, accessibility by ROV was limited, and the precise extent of the concrete erosion outside of the pedestal area could not be

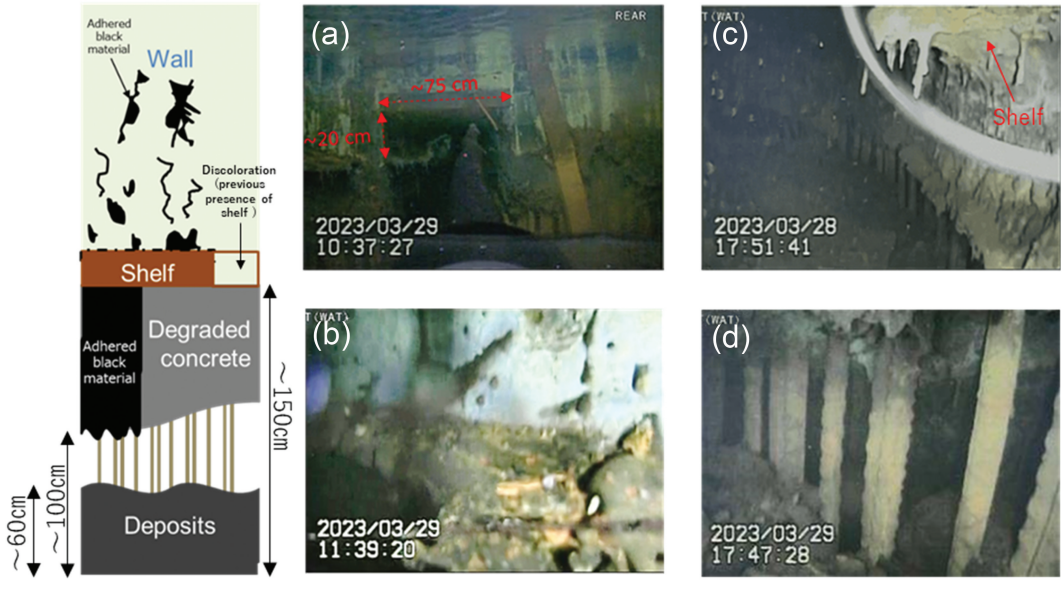

Fig. 11. Left: vertical distribution of wall states. (a) State difference above and below shelf level around the pedestal opening (E-3). (b) Dark materials attached to the wall and accumulated on the shelf (NNE-3). (c) Concrete degradation below the shelf level (E-3 to ENE-3). (d) Exposed rebar and lower deposits bed (NE-3).

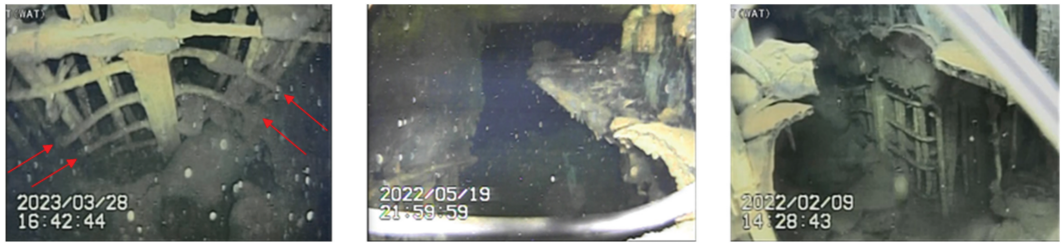

Fig. 12. State of pedestal opening. (a) Left wall with exposed inner skirt and rebar. (b) Upper part with shelf deposit. (c) Outer right corner with exposed rebar and shelf deposits. Red arrows are pointing at bent rebars.

confirmed. A decreasing trend of the concrete erosion height was observed with increased distance from the pedestal opening.

Through previous PCV internal investigation efforts, in which a camera was suspended through the grating from the floor above, it became apparent that a high volume of deposits of unknown nature is present in the D/W annulus.[6] The results of detailed inspection utilizing ultrasonic waves indicate that the height of deposits decreases with increased distance from the pedestal opening at ~170 deg except for the area right in front of this opening (Fig. 13). By comparing the recently obtained information with the estimated height of deposits from 2017, it became apparent that no significant redistribution of materials occurred between the two separate investigations. The maximum height of deposits outside of the pedestal area was evaluated to be ~1.1 m based on ultrasonic wave analysis and ~1.3 m (on the outer edge of the pedestal opening) based on visual information. The height of the deposits was evaluated to be ~0.2 m from the original floor level at the minimum. Some of the deposits overcame the lower edge of the torus downcomer about 20 cm high from the floor level, and a currently unknown volume of materials relocated behind jet deflectors F, E, and D, which are located nearest to the pedestal opening (Fig. 14). The state of the original D/W floor could not be observed at any of the investigated areas.

At least in part of the investigated area, large cavities exist below the surface level of the deposits, which similarly as in the pedestal area and in the pedestal opening form the so-called shelves. At this point, the extent of the cavities remains unknown. Shelf deposits were observed particularly inside the pedestal opening on the north wall, between the outer side of the pedestal wall, piping of the primary loop recirculation system (PLR), the D/W shell, jet deflector E, and shielding block of the equipment drain sump pump at the height of ~1 m, as seen in Fig. 13. Based on the shape of the deposits piled between the pedestal opening and the D/W shell, it is assumed that part of them are collapsed fragments of the shelves.

Height gradient and ripplelike patterns can be observed on the upper surface of these shelves (Fig. 15), while the

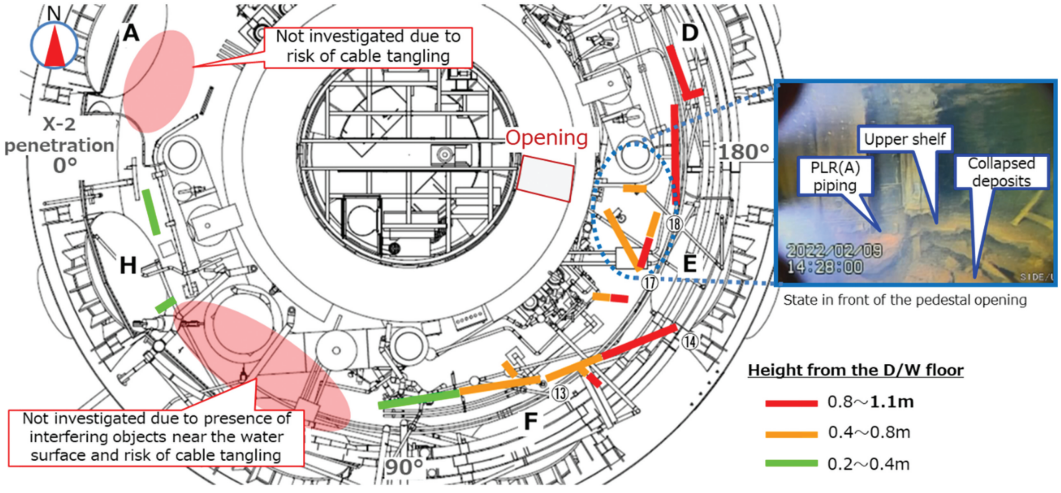

Fig. 13. Height distribution of the deposits.

Fig. 14. Clogging of the bottom openings of vent pipe behind jet deflector E (ENE-6).

bottom side, especially in and near the pedestal opening, has "lavacicle"-like formations (Fig. 16). The thickness of the shelf was estimated to be 3 to 4 cm both near the pedestal wall (Fig. 15) and near the D/W shell, with similar high porosity observed on the profile in both cases. Between the PLR piping and the D/W shell and jet deflector E, a second layer of shelf was observed, with its surface being relatively flat, in contrast to the wrinkly shape of the upper shelf. These two layers are interconnected along the D/W shell, and some metallic support structures are entrained in between them, without any observable damage or deformation along their length (Fig. 17).

The observed damage to the preexisting structures is limited to the RCW piping that could not be confirmed along the outer pedestal wall, where it was originally installed (135 to 170 deg), and some small-sized piping located at a low height from the original D/W floor in front of the pedestal opening. In contrast, multiple support structures and pipes standing vertically in front of the pedestal wall are only slightly deformed both below and above the height of the shelf deposits (Fig. 18). Similarly, no obvious deformation or melting was confirmed on the PLR piping or shielding block of the equipment drain sump pump or jet deflectors.

Besides the shelf deposits, other deposits of various shapes, sizes, and distributions have been confirmed, including bulky round deposits, threadlike deposits, thin layered spherical deposits resembling eggshells, and glossy glasslike deposits near the pedestal opening. Since materials of unknown nature were also found suspended on the structures high above the water level, it is expected that part of the materials currently piled on the D/W floor came from upper floors of the D/W. Among these, deposits thought to be molten and resolidified lead of the PLR piping shielding blankets were found on top of the other deposits both near the pedestal opening (180 deg) and in the opposite side of the D/W, near the ROV insertion point (0 deg). Although the height of the deposits differs in both locations (~1 and 0.2 m, respectively), the height of the failure of the silicone fiberglass fabric blankets is about 1.2 m regardless of the location in the D/W. Moreover, this height seems to be the same as that of discoloration found along the D/W shell and metallic structures in the entire investigated scope of the D/W annulus, considered to be a trace of the water level that was kept relatively constant shortly after effective water injection into the PCV was established in 2011. Other materials with relatively low melting point that are largely abundant in the D/W are insulation casing of the RCW piping made of aluminum, existing both below and above the current water level (~2.0 m). Although some damage was confirmed to these casings, this was limited to only the area near the vicinity of the equipment drain sump (135 deg) and not in the entire area of the D/W.

Fig. 15. Wrinkly shape of the upper surface of shelf deposits (SE-6) and porosity observed on the fragmented side (E-4).

Fig. 16. Lavacicles on the bottom side of the shelf at the corner of pedestal opening.

III. DISCUSSION OF UNIT 1 ACCIDENT PROGRESSION AND POSSIBLE SCENARIOS

The reactor was successfully scrammed and subsequently cooled using the passive isolation condenser system (IC) after the earthquake. To keep the cooling and depressurization rate of the reactor within the range prescribed by the operational procedures, the operators operated the valves of the IC to open and close multiple times until the arrival of the tsunami. Since all the power sources were lost practically immediately after the tsunami struck the site, the valves became inoperable and remained in the closed position that they were currently in, rendering the reactor core uncooled. Although operators attempted to establish alternative water injection measures, these efforts are generally agreed upon to have been unsuccessful. Because of the loss of all power, only very scarce information is available regarding the RPV and PCV water levels, temperatures, and pressures, bringing a high degree of uncertainty into the accident progression analysis.

The most recent estimates based on both simulation results and the plant data collected at the time of the accident assume the start of core damage about 4 h, the beginning of core slumping about 11.5 h, and RPV failure with subsequent debris relocation to the pedestal area about 15.5 h after scram. A huge mass of molten materials including molten fuel and reactor internals amounting to some 140 tons is assumed to relocate ex-vessel in a short span of about 30 min under the low RPV pressure condition. The ex-vessel progression developed for about 11 days under a dry cavity condition since effective water injection into the RPV could not be established until March 23, despite continuous efforts of the operators.[6] Although a high degree of uncertainty is present, it is considered to be a plausible scenario and within the range of results obtained from the benchmarking exercises of the Benchmark Study of the Accident at the Fukushima Daiichi Nuclear Power Station project (OECD/NEA joint project).[9,10]

III.A. RPV LH Failure and Transition to Ex-Vessel Phase

It is difficult to assess the leading LH failure mechanism of the boiling water reactor (BWR) such as its geometrically complicated structure including multiple penetrations and presence of various types of materials, such as weld-overlay cladding, control rod guide tubes, stub tubes, welds, etc. Depending on the development of the in-vessel phase, three main failure modes, namely,

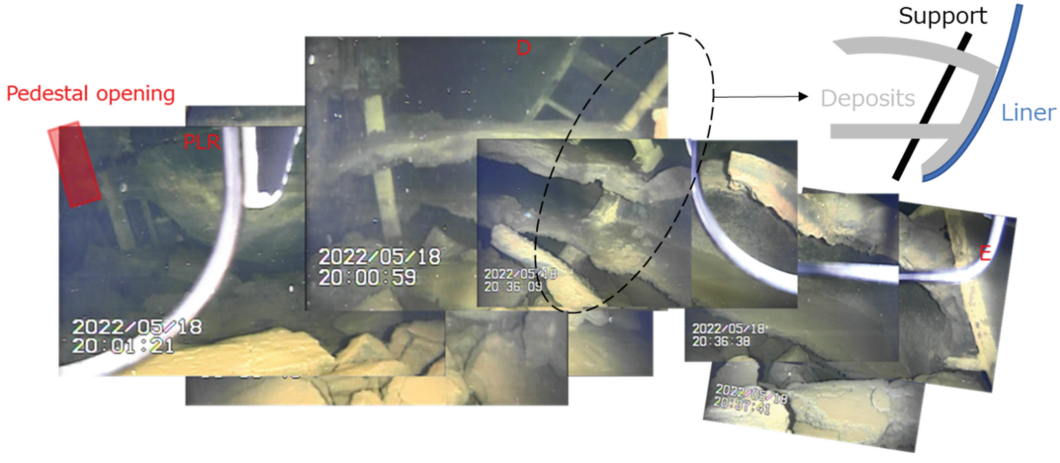

Fig. 17. Shelf deposits reaching from the right corner of the pedestal opening, along PLR piping, toward the D/W shell and jet deflectors D, E (E-4 to 6 to ESE-4 to 6).

penetration tube ejection, tube heatup and failure, and global rupture, are considered.[19,20] Although the the LH could not be observed directly, because of the limitations of the investigation tools and the conditions inside the pedestal area, some indirect information regarding the current state of the LH can be drawn. From the observations described in Secs. II.A and II.B, it is apparent that multiple failure openings exist in the LH, based on the facts that cooling water dripping from above was confirmed in multiple locations and multiple CRD and ICM housings relocated into the lower parts of the pedestal area.

The vulnerability of CRD housings and stub tubes to eutectic melting caused by a Zr-rich liquid metal pool and the possibility of molten metal intrusion into the CRD housings has been previously studied.[21] On the other hand, even if the welded part of the CRD housing penetration failed, large deformation of the vessel due to creep would be needed for the CRD to be ejected.[22] Nevertheless, in the case of BWRs, the CRD housing is prevented from fully ejecting from the RPV by the support structure below the LH, by leading the housing to the grid clamp where it rests. Gross release of debris in such a case might not occur, although gas blowdown can be expected. Clogging of the inner parts of some CRD housings by debris as well as the shape of the top end of the housing being at an angle of about 45 deg (Figs. 4 and 8) could be caused by the melting of the part of CRD housing and stub tube within the RPV in line with the shape of the LH in its outer periphery and falling of CRD housing after the support structure outside the RPV was damaged or overloaded. On the other hand, the ICM housings are not supported by the above-mentioned support grid; therefore, the failure of the ICM housing weld could lead to immediate ejection of the tube creating a pathway for the ex-vessel relocation of molten materials with a relatively small diameter, which could be further expanded by ablation caused by outflow of debris.

In the recent investigation, one ICM housing apparently detached from the LH was found suspended above the water level in the outer periphery of the pedestal area (Fig. 5). Because the observed ICM housing is clearly lower than its original position yet it is not supported from below, it is assumed that some of its upper part is stuck in the dense array of other structures and/or solidified debris retained in the areas that could not be directly observed at this time. The fact that multiple CRD housings are found on top of the deposits in the pedestal area or partially buried in them might suggest their relocation in the later stage of the ex-vessel phase (Fig. 4). It is also unclear whether some other relocated housings are buried under the deposits or completely melted.

The possibility of molten material intrusion into the instrument tubes and failure of the tube outside of the vessel wall has been raised too.[23] It can be expected that a metallic pour would eventually freeze and plug the instrument tube without causing it to melt, but the mechanical loads under elevated temperatures could result in creep rupture of the tube after bottom head dryout in an unmitigated BWR severe accident. Such failure can be expected in the hottest central area of the LH. Another potential location of such creep failure caused by intrusion of melt is the RPV drain line penetration in the center of the LH (Ref. 20).

Global failure under the depressurized RPV condition could take place after dryout and debris bed reheating, long after the penetration failures, but would provide for the largest ex-vessel relocation path of the three considered scenarios. The positional relationship of the CRD housing flanges observed in the upper pedestal region, which seems to be not significantly deviating from their original vertical position but misaligned from their horizontal pitch (Fig. 9), might be a sign of a larger-scale rupture of the LH, i.e., vessel sag or "unzipping." Moreover, some of the CRD housings (length of ~4 m) were found rotated upside down, which would require a high degree of damage especially in the central area to allow for such movement (Fig. 6).

Bulky deposits attached to the relocated CRD housings, especially in the upper locations, can be considered solidified debris (Fig. 10). Because of the high number and dense pitch of CRD housings, temporary freezing of corium outside of the RPV and significant retention in this area could happen prior to the detachment of the housings from the RPV. Further retention and eventual collapse or melting of CRD exchange equipment would practically change the melt composition, adding several tons of metallic materials and practically decreasing the average temperature of the melt. These events would significantly affect the later ex-vessel development.

At this point, a single mechanism cannot be pointed out (or ruled out) as the dominant one leading to rapid relocation of molten materials into the pedestal. It is possible that multiple mechanisms were taking place in parallel or subsequently with the order of events also remaining unclear at this point. Further investigations of the upper pedestal area as well as the RPV internal regions are expected to bring more information on size and location of the LH breach(es).

III.B. Concrete Erosion (MCCI)

The erosion of concrete structures on the D/W floor is something to be expected given the severity of the accident progression and failure of mitigation measures at Unit 1. The relatively uniform height up to which the concrete eroded inside the pedestal area (Fig. 3) and in the pedestal opening (Fig. 12) suggests spread of the corium over the entire floor of the cavity before any significant erosion took place, which is consistent with rapid high-temperature melt pour scenarios. Moreover, decreasing erosion height with increasing distance from the pedestal opening in the D/W annulus area (Fig. 18) would be consistent with an expected decrease in height of the melt in the tangential direction outside of the opening but is in contrast with the wide distribution of deposits.

As a result of this concrete erosion, the support structures originally embedded in the pedestal wall (i.e., rebars and inner skirt) were exposed, and their current state is largely sound (Figs. 11d and 12). This conflicts with the expectations coming from the MCCI knowledge accumulated up to date, which expects the rebar mesh to be eroded together with the concrete.[8] Although some experiments were conducted in recent years to investigate the potential effect of rebars on the ablation front progression,[24] clean separation of concrete without damage to rebars was not deemed realistic. Long-term effects, such as coolant water flow and slow degradation over the period of 12 years (similar to leaching) after the accident, offer themselves as seemingly plausible explanations, but the bending of horizontal rebars welded to the inner skirt (Fig. 12) implies that such long-term degradation was not the main contributor. These rebars are thought to have bent under their own weight as a result of the increased temperature causing the deterioration of their mechanical properties. In the longer term, when the flow of cooling water could cause the degradation of the concrete, the temperature inside the PCV is considered to be too low to significantly affect the mechanical properties of steel. It seems likely that the temperature to which the rebars were exposed was simply not sufficient to cause their melting but was high enough for the concrete matrix to erode and for horizontal rebars to lose their mechanical strength and to bend under their own weight.

Spalling, a frequently observed phenomenon resulting from quick and prolonged exposures of concrete to high temperatures (such as fires), was considered to play only a minor role in MCCI. However, the possibility of a certain combination of conditions enhancing the importance of spalling within MCCI might be worth considering. Factors playing an important role include number of heated surfaces and presence or absence of reinforcement, stress, thickness, moisture content, aggregate and reinforcement expansion, etc.[25] The recent observations of the pedestal wall state raise a reason for further examination of the potential role of spalling in the development of concrete erosion as a part of the MCCI phenomena.

From the observations inside the pedestal area and the pedestal opening, it became clear that the height of concrete erosion is below the height of the shelf deposits and about the same as the height of the inner skirt, or a few centimeters higher at the local maxima. The possibility of the inner skirt contributing to the development of concrete erosion must be examined. Because of the positional relationship within the PCV and pedestal wall, it can be expected that the inner skirt could come into contact with high-temperature materials relatively early after the beginning of the ex-vessel phase.

One of the likely points of early contact is inside the pedestal opening, where the inner skirt has no concrete overlay. The other possibility to consider is the enhanced spreading of the ablation front inside the sump pits, where the depth of the molten materials would be 1 m higher than in the rest of the pedestal area resulting in more challenging coolability of such configuration. Given that the edge of the sump pit and the surface of the inner skirt are separated by approximately 75 cm of concrete (Fig. 2), it is possible that the ablation front reached the surface of the inner skirt in this area earlier than in other locations. Thanks to the high thermal conductivity of the inner skirt (compared to that of concrete), the heat could be transferred to the center of the pedestal wall in a relatively short period of time, without reaching temperatures that would result in melting or plastic deformations. Heatup of the pedestal wall from inside and mechanical stresses associated with the thermal expansion of the skirt in combination with the heat being transferred from the corium directly to the pedestal wall surface could contribute to relatively homogeneous height of concrete erosion inside the pedestal area. The asymmetry of concrete erosion height and its gradient on the outer wall of the pedestal near the opening (Figs. 18 and 19) could be caused by the more severe conditions in the vicinity of the equipment drain sump pit (SE). However, since the outside of the pedestal wall near the floor drain sump pump (NW) is not eroded, it seems to be highly probable that there were multiple factors causing the concrete to erode. In combination with the corium spread into the D/W annulus in the vicinity of the pedestal opening, the conditions could be created for the concrete erosion of the outer wall in the limited extent.

The existence of shelves could be linked to phenomena frequently observed in MCCI experiments, referred to as

Fig. 18. Erosion height gradients and state of the structures on the outer sides of the pedestal opening (covered by a pink sheet in the central picture); yellow lines mark parts considered to be remaining concrete below the shelves; numbers in red circles indicate original structures that could be identified.

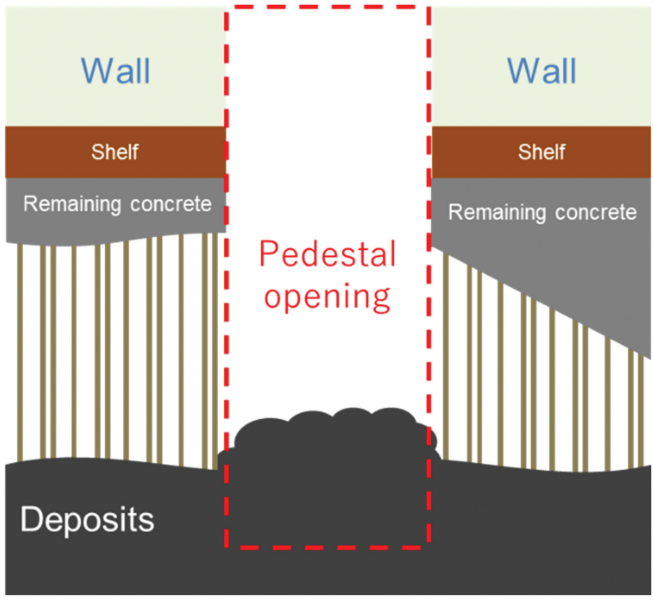

Fig. 19. Illustration of the wall states on both sides of the pedestal opening as seen from the outside (structures and horizontal rebars omitted).

anchoring. Anchoring was deemed to be an undesired effect coming from the limitations of experimental setups, where the rather narrow geometry of the cavity could result in the floating crust freezing on the side walls, thus preventing intrusion of cooling water. Large-scale crust anchoring was considered unattainable in the actual plant condition, given the insufficient mechanical strength of the prototypic crust.[26] The edges of the shelves observed inside the pedestal (Fig. 11) seem to be generally round without showing signs of larger shelves breaking (except for the areas near the wall apparently broken by the fallen CRD housings) unlike in the area outside of the pedestal (Fig. 17). This suggests that an anchored crust was not spanning across the entire pedestal area. Moreover, in the area outside of the pedestal, the shape of the collapsed fragments suggests that the covered area was limited only to the vicinity of the structures that could act as local heat sinks (i.e., D/W shell, jet deflector, shielding block, PLR piping, pedestal wall, and others), causing the solidification and attachment of the materials.

Regarding the dark black materials adhering to some parts of the walls inside the pedestal and in the pedestal opening above the level of the concrete erosion, their nature and origin are not fully understood at this moment. One plausible explanation could be that these materials are results of "volcanic" eruptions caused by decomposition gases entraining melt droplets.[7] Similarly, "icicles" found on the bottom side of some shelves (Fig. 16) could be formed with solidification of the entrained melt as it was dripping from the solid shelf.

Although the axial erosion of the D/W floor concrete could not be investigated to this day, the water leaking from the sand cushion drainpipe under the D/W shell points at the possibility of shell damage.[6] However, since the relatively high level of water can be maintained in the D/W and another leak point on the expansion joint of the vacuum breaker line in the torus room was confirmed as well, it is probable that damage to the D/W shell is minor, if any. Similarly, at this point, no information is available on ablation profile and potential stratification of the steel and oxide phases.

III.C. Distribution and Height of Deposits

The height distribution of deposits in the D/W annulus (Fig. 13), where the maximum is evaluated to be about 1.3 m from the original D/W floor, is in contrast with the height estimated assuming that all the molten material inventory piles up only within the pedestal area. This would result in a height of about 1.1 m. The estimation did not take the porosity and presence of equipment inside the pedestal into account since they are unknown, which effectively decreases the estimation results. On the other hand, the volume of sump pits was excluded from the evaluation, and melting of all reactor core and internals, including the shroud and its dome flange, is considered to give a sufficiently conservative result. If the same volume was to be spread evenly in the pedestal area (~20 m^2) and the D/W annulus (~90 m^2), the spread height would not exceed 0.2 m.

Generally, with a rapid pour of high-temperature low-viscosity melt into the dry cavity, practically instant spread of corium over the entire floor of the cavity (pedestal area) can be expected. However, modeling of spreading over the D/W annulus floor predicts quite different behavior depending on the melt pour conditions,[27] and consideration of equipment posing as obstacles and concurrent complex interactions with the construction materials is overly simplified in these models. Because of the presence of cavities below the shelves, the height distribution itself might not be representative of the volume of the materials relocated from the RPV and could be a trace of the transients during concrete ablation or spreading.

A possible explanation for the presence of cavities and morphology of the deposits is formation of viscous skin[28] on the surface of the hotter molten debris, which keeps forming and freezing on relatively cold surfaces in the process of the debris spreading. Such phenomena

were observed in volcanic activities and are referred to as Pahoehoe or ropy lava, leading to formation of lava tubes in some cases.[29] After the breakout of molten materials from the pedestal opening, these would move in the radial direction toward the D/W shell and jet deflector E, potentially overflowing the lower edge of the vent pipe, with some of the materials farther relocating toward the suppression chamber (S/C). It was confirmed that the lower gaps of jet deflectors D, E, and F are clogged with solidified materials (Fig. 14). After freezing of the materials in these relocation paths, the only free paths for the materials to further relocate would be in the tangential directions, resulting in a relatively even spread of materials over the entire D/W below the lowest height of the vent downcomer pipe (~20 cm) if the viscosity of the melt would be sufficiently low.

With the progression of concrete erosion, especially in the pedestal area, and mixing of concrete constituent materials, the liquidus and solidus temperatures decrease, creating favorable conditions for further relocation. Furthermore, melt swelling or foam formation caused by the gases generated during the concrete ablation can result in some regions of the melt to raise in height and to subsequently separate from the melt pool in the later phases when the gas sparging is reduced, creating cavities.[30] High porosity observed on the fragmented shelves further supports this hypothesis, and the wrinkly patterns observed on the surfaces of the upper shelves (Fig. 15) are in support of the hypothesis that these were formed in the process of the spreading, while the relatively flat surface of the lower shelf is indicative of its formation at the time when the spreading practically ceased and the separation from the lower debris bed could be caused by the axial ablation and/or shrinking of the debris with its cooldown.

Besides the pedestal opening as the main relocation pathway, opening on the upper floor used for the replacement of CRDs during the maintenance operations can be considered as another potential relocation path because a bundle of CRD housings was found inside the pedestal area partially stuck in this opening (Fig. 10) and some of the deposits were found outside the pedestal area suspended on pipes and structures in elevated locations. Although this material relocation path is not considered to be a major one, interaction with various materials (ducts, gratings, cabling, insulation, etc.) along the relocation path could be the reason for the existence of some characteristic morphology of deposits in limited areas below this opening (SE-4, SSE-4) while the observed higher local pileup of deposits could be caused by their accumulation on top of the deposits that previously relocated through the pedestal opening on the D/W floor level.

At this point, the detailed composition of bulk deposits inside and outside the pedestal area remains unknown. More advanced sampling and analyses to be conducted in the future are expected to bring information on detailed composition, and attention should be given in particular to the content of concrete-constituting materials and fuel materials. Grasping the differences in composition will provide more information on the progress and timing of the materials spreading.

III.D. State of the Structures in D/W Annulus

While the degree of damage to the equipment inside the pedestal area is remarkable, with practically no parts of the CRD exchange equipment remaining, the damage to the metallic structures outside of the pedestal area is limited only to the vicinity of the pedestal opening in spite of the deposits being present in practically the entire area of the D/W. Damage to the piping of the RCW in the pedestal and/or in the vicinity of the pedestal opening resulted in a high degree of contamination of parts of the RCW outside of the PCV, such as the heat exchangers and surge tank. Although the piping was not found in its original location near the D/W floor, the vertically rising part of the pipe near the equipment drain sump pump is still present, although damage to its insulation was confirmed.

Similarly, some other pipes of small diameter that were originally located at a relatively low height from the floor could not be found. On the other hand, some other metallic structures in the same area could be found in their original location despite part of them being enclosed between the lower debris bed and the shelf deposits (Fig. 18). This might suggest relatively low temperature to which these were subjected in the elevated areas and the most severe thermal conditions in relatively low height from the D/W floor.

Similarly, the state of PLR piping, support structures, and jet deflector plates between the shelves and lower debris bed is fundamentally intact (Fig. 17). In the BWR Mark I, attack of the melt on the D/W shell without any interventions (such as D/W spray, etc.) is expected to result in early failure of the containment, bypass of the S/C, and a catastrophic release of the contaminants into the environment.[31] Since a high level of water can be maintained in the D/W and most of the metallic structures in the outer circumference of the D/W annulus are relatively intact, failure of the D/W shell seems to be improbable.

These observations further support the hypothesis that the relocating materials that reached the D/W shell and vast area of the D/W annulus did so when their temperature was significantly lower than the temperature of the materials right after relocation from the RPV LH. The extent to which the high-temperature materials spread right after the LH failure could be limited to the pedestal area and vicinity of the pedestal opening. After some retention inside the pedestal area accompanied by concrete erosion and melting of the metallic structures inside the pedestal, this bulk mass could break away through the pedestal opening and spread farther away under significantly altered conditions, including temperature, composition, and viscosity.

From the state of other metallic structures in the D/W annulus, global temperatures in the PCV can be deducted. Melting of the lead shielding in practically the entire area of the PCV means that the temperature exceeded 327.5°C globally but remained below 660°C since the damage to the insulation covers made of aluminum is limited only to the RCW piping leading to/from the equipment drain sump pit. This is further supported by the D/W temperature measurement data, which became available after March 20, 2011, when the first measured temperature in the D/W became available. Values for most of the thermometers showed temperatures near 400°C, which is the upper range of the measurement devices used.

The constant height of failure of the lead shield blankets for both PLR piping systems A and B regardless of the height of deposits in the vicinity but in correlation with the height of discoloration on the metallic structures implies that this failure was caused not by the heat of the relocated materials but rather by the water chemistry shortly after effective water cooling into the containment was established. Moreover, the fact that the relocated lead could be found on top of the deposits or shelves means that their failure occurred after the materials were already spread widely around the D/W.

IV. CONCLUSIONS

Through the careful analysis of data obtained in the most recent PCV internal investigations at Unit 1, the current state of the equipment and distribution of deposits could be grasped to a big extent. This information is crucial for planning the next steps in decommissioning work as well as clarifying the accident progression. Although more information, including visual inspections inside of the RPV, composition analyses of deposits, etc., will be necessary to describe the events in more detail, some valuable information to serve as a basis for the discussion has been obtained already. The main findings can be summarized as follows:

1. Multiple failure openings presumably exist in the RPV LH as multiple CRD housings were relocated within the pedestal.

2. The equipment inside the pedestal area (i.e., CRD exchange equipment) was largely damaged by the relocated materials to the extent that practically no parts are remaining/can be identified. The damage to the pre-existing structures outside of the pedestal area is limited to the vicinity of the pedestal opening.

3. The concrete of the pedestal wall is eroded to the height of about 1 m along the inner circumference of the pedestal and to a limited extent on the outer side of the pedestal. The reinforcing structures (rebars and inner skirt) are largely intact.

4. Deposits are present in the entire area of the D/W floor, with height distribution between 1.5 m at maximum and 0.2 m at minimum, reaching into the vent pipes connecting the D/W with the wetwell (the extent of this spread remains unconfirmed).

5. Cavities could be confirmed below the shelf deposits attached to the concrete and metallic structures (PLR piping, jet deflectors, D/W shell, etc.).

6. No obvious thermal damage to the D/W shell could be observed despite its contact with the deposits.

In general, when discussing the observed facts, it must be kept in mind that more than 10 years have passed since the situation had been largely stabilized; therefore, the effect of time; cooling water flow; and external events, such as earthquakes, could have significantly altered the distribution and state of the materials in the PCV.

The main topics to be addressed in future research to satisfyingly explain the observations can be summarized as follows:

1. Identification of the dominant mode and location of the LH failure.

2. Consideration of complex geometry of the upper pedestal region with including the possibility of temporary freezing and retention of molten materials on the CRD housings or CRD exchange equipment.

3. Concrete erosion mechanism without thermal damage to the reinforcing structures (i.e., rebars and inner skirt), including the possibility of concrete erosion under relatively low temperatures.

4. Role of heat conduction in concrete and reinforcing metallic structures.

5. Spreading behavior with consideration of mixing of materials coming from concrete erosion and preexisting structures acting as obstacles and heat sinks.

6. Distribution of fuel materials within the large volume of deposits both in the pedestal area and in the D/W annulus.

The above-mentioned topics are to a large extent intrinsically interconnected, and to comprehensively explain the events that took place in the RPV and PCV of Unit 1 in 2011, further site inspections as well as experimental programs and analyses will be required. Hence, it can be expected that many of the questions raised in this paper will be elucidated in the future, leading to better understanding of the relevant phenomena, further improvement of severe accident codes, and increased levels of nuclear safety for both operating reactors and newly planned designs.

Acronyms

BWR: boiling water reactor
CRD: control rod drive
D/W: drywell
E: east
ENE: east-northeast
ESE: east-southeast
IC: isolation condenser system
ICM: in-core monitor
LH: lower head
MCCI: molten core–concrete interaction
N: north
NE: northeast
NNE: north-northeast
NNW: north-northwest
NW: northwest
OECD/NEA: Organisation for Economic Co-operation and Development/Nuclear Energy Agency
PCV: primary containment vessel
PLR: primary loop recirculation system
RCW: reactor building closed cooling water system
ROV: remotely operated vehicle
RPV: reactor pressure vessel
S/C: suppression chamber
S: south
SE: southeast
SSE: south-southeast
SSW: south-southwest
SW: southwest
TEPCO: Tokyo Electric Power Company
W: west
WNW: west-northwest
WSW: west-southwest

Acknowledgments

The content of this material includes output of the Ministry of Economy, Trade and Industry subsidy for Project of Decommissioning and Contaminated Water Management (Development of Technologies for Detailed Investigation inside PCV).

Disclosure Statement

No potential conflict of interest was reported by the author(s).

ORCID

Shinya Mizokami http://orcid.org/0000-0002-0971-5649

References

1. M. PELLEGRINI et al., "Confirmation of Severe Accident Code Modelling in Light of the Findings at Fukushima Daiichi NPPs," *Nucl. Eng. Des.*, **354**, 110217 (2019); https://dx.doi.org/10.1016/j.nucengdes.2019.110217.

2. Y. YAMANAKA et al., "Update of the First TEPCO MAAP Accident Analysis of Units 1, 2, and 3 at Fukushima Daiichi Nuclear Power Station," *Nucl. Technol.*, **186**, *2*, 264 (2014); https://dx.doi.org/10.13182/NT13-46.

3. L. ALBRIGHT et al., "U.S. Efforts in Support of Examinations at Fukushima Daiichi—November 2022 Meeting Notes and Information Request Status," ANL-22/85, Argonne National Laboratory (Apr. 2023).

4. J. REMPE et al., "Revisiting Insights from Three Mile Island Unit 2 Postaccident Examinations and Evaluations in View of the Fukushima Daiichi Accident," *Nucl. Sci. Eng.*, **172**, *3*, 223 (2012); https://dx.doi.org/10.13182/NSE12-3.

5. H. FUJII et al., "Investigation of the Unit-1 Nuclear Reactor of Fukushima Daiichi by Cosmic Muon Radiography," *Prog. Theor. Exp. Phys.*, **2020**, *4* (2020); https://dx.doi.org/10.1093/ptep/ptaa027.

6. "The 6th Progress Report on the Investigation and Examination of Unconfirmed and Unsolved Issues on the Development Mechanism of the Fukushima Daiichi Nuclear Accident," Tokyo Electric Power Company Holdings, Inc.; https://www.tepco.co.jp/en/hd/decommission/information/accident_unconfirmed/index-e.html (current as of Jan. 1, 2024).

7. M. T. FARMER, D. J. KILSDONK, and R. W. AESCHLIMANN, "Corium Coolability Under Ex-Vessel Accident Conditions for LWRs," *Nucl. Eng. Technol.*, **41**, *5*, 575 (2009); https://dx.doi.org/10.5516/NET.2009.41.5.575.

8. J. M. BONNET et al., "State-of-the-Art Report on Molten Corium Concrete Interaction and Ex-Vessel Molten Core Coolability," NEA No. 7392, Organisation for Economic Co-Operation and Development/Nuclear Energy Agency (2017).

9. M. PELLEGRINI et al., "Main Findings, Remaining Uncertainties and Lessons Learned from the OECD/NEA BSAF Project," *Nucl. Technol.*, **206**, *9*, 1449 (2020); https://dx.doi.org/10.1080/00295450.2020.1724731.

10. L. E. HERRANZ et al., "Overview and Outcomes of the OECD/NEA Benchmark Study of the Accident at the Fukushima Daiichi NPS (BSAF) Phase 2—Results of Severe Accident Analyses for Unit 1," *Nucl. Eng. Des.*, **369**, 110849 (2020); https://dx.doi.org/10.1016/j.nucengdes.2020.110849.

11. M. PELLEGRINI et al., "Analysis of the Long Term Interaction Between Molten Core and Dry Concrete at Fukushima Daiichi Unit 1," presented at 20th Int. Topl. Mtg. Nuclear Reactor Thermal Hydraulics (NURETH 20), Washington D.C. August 20–25, 2023.

12. "2022.2.8 Implementation Status of the Unit 1 Primary Containment Vessel Internal Investigation (from Investigation on February 8) at the Fukushima Daiichi Nuclear Power Station," Tokyo Electric Power Company Holdings, Inc.; https://www4.tepco.co.jp/en/news/library/archive-e.html?video_uuid=j295y47o&catid=61785 (current as of Jan. 1, 2024).

13. "2022.2.9 Implementation Status of the Unit 1 Primary Containment Vessel Internal Investigation (from Investigation on February 9) at the Fukushima Daiichi Nuclear Power Station," Tokyo Electric Power Company Holdings, Inc.; https://www4.tepco.co.jp/en/news/library/archive-e.html?video_uuid=hjo1v4ul&catid=61785 (current as of Jan. 1, 2024).

14. "2022.03.24 Implementation Status of Unit 1 Primary Containment Vessel Internal Investigation (ROV-A2) (Work Conducted Between March 14~16) at the Fukushima Daiichi Nuclear Power Station," Tokyo Electric Power Company Holdings, Inc.; https://www4.tepco.co.jp/en/news/library/archive-e.html?video_uuid=yw0uzql2&catid=61785 (current as of Jan. 1, 2024).

15. "2022.05.23 Implementation Status of the Unit 1 Primary Containment Vessel (PCV) Internal Investigation (ROV-A2) (Work Conducted Between May 17~19)," Tokyo Electric Power Company Holdings, Inc.; https://www4.tepco.co.jp/en/news/library/archive-e.html?video_uuid=sd7bw090&catid=61785 (current as of Jan. 1, 2024).

16. "2023.04.04 Implementation Status of the Unit 1 Primary Containment Vessel (PCV) Internal Investigation (ROV-A2) (Work Conducted Between March 28~30, 2023)," Tokyo Electric Power Company Holdings, Inc.; https://www4.tepco.co.jp/en/news/library/archive-e.html?video_uuid=14952&catid=61785 (current as of Jan. 1, 2024).

17. T. YAMASHITA et al., "Comprehensive Analysis and Evaluation of Fukushima Daiichi Nuclear Power Station Unit 2," *Nucl. Technol.*, **206**, *10*, 1517 (2020); https://dx.doi.org/10.1080/00295450.2019.1704581.

18. T. YAMASHITA et al., "Comprehensive Analysis and Evaluation of Fukushima Daiichi Nuclear Power Station Unit 3," *Nucl. Technol.*, **209**, *6*, 902 (2023); https://dx.doi.org/10.1080/00295450.2022.2157663.

19. S. A. HODGE, "BWR Reactor Vessel Bottom Head Failure Modes," CONF-890546-3, Oak Ridge National Laboratory (1989).

20. J. L. REMPE, S. A. CHAVEZ, and G. L. THINNES, "Light Water Reactor Lower Head Failure Analysis," NUREG/CR-5642; EGG-2618, U.S. Nuclear Regulatory Commission (Oct. 1993).

21. T. YAMASHITA et al., "BWR Lower Head Penetration Failure Test Focusing on Eutectic Melting," *Ann. Nucl. Energy*, **173**, 109129 (2022); https://dx.doi.org/10.1016/j.anucene.2022.109129.

22. F. SCARPA, M. PELLEGRINI, and M. NAITOH, "Validation of Severe Accident Code SAMPSON Debris Cooling Analysis Module (DCA) Against OLHF Experiments and Development of Creep Models," presented at 11th Int. Topl. Mtg. Nuclear Reactor Thermal Hydraulics, Operation and Safety (NUTHOS-11), Gyeongju, Korea, October 9–13, 2016.

23. M. NAITOH et al., "Melting Test of Penetrating Tube Through BWR-RPV Bottom Wall," *Ann. Nucl. Energy*, **173**, 212 (2018); https://dx.doi.org/10.1016/j.anucene.2018.03.034.

24. J. J. FOIT et al., "MOCKA-SSM Experiments on Basaltic Concrete with and Without Rebars," presented at 12th Int. Topl. Mtg. Nuclear Reactor Thermal Hydraulics, Operation and Safety (NUTHOS-12), Qingdao, China, October 14–18, 2018.

25. R. JANSSON, "Fire Spalling of Concrete: Theoretical and Experimental Studies," PhD Thesis, KTH Royal Institute of Technology (2013).

26. S. LOMPERSKI and M. T. FARMER, "Corium Crust Strength Measurements," *Nucl. Eng. Des.*, **239**, *11*, 2551 (2009); https://dx.doi.org/10.1016/j.nucengdes.2009.06.013.

27. M. T. FARMER, K. R. ROBB, and M. W. FRANCIS, "Fukushima Daiichi Unit 1 Ex-Vessel Prediction: Core Melt Spreading," *Nucl. Technol.*, **196**, *3*, 446 (2016); https://dx.doi.org/10.13182/NT16-44.

28. C. JOURNEAU et al., "Ex-Vessel Corium Spreading: Results from the VULCANO Spreading Tests," *Nucl. Eng. Des.*, **223**, *1*, 75 (2003); https://dx.doi.org/10.1016/S0029-5493(02)00397-7.

29. J. H. FINK and R. C. FLETCHER, "Ropy Pahoehoe: Surface Folding of a Viscous Fluid," *J. Volcanol. Geotherm. Res.*, **4**, *1–2*, 151 (1978); https://dx.doi.org/10.1016/0377-0273(78)90034-3.

30. B. TOURNIAIRE, E. DUFOUR, and B. SPINDLER, "Foam Formation in Oxidic Pool with Application to MCCI Real Material Experiments," *Nucl. Eng. Des.*, **239**, *10*, 1971 (2009); https://dx.doi.org/10.1016/j.nucengdes.2009.05.001.

31. T. G. THEOFANOUS, H. YAN, and M. Z. PODOWSKI, "The Probability of Mark-I Containment Failure by Melt-Attack of the Liner," NUREG/CR-6025, U.S. Nuclear Regulatory Commission (Nov. 1993).